

**Use of NASA A-Train and NAMMA Observations to
Evaluate a New Dust Source Scheme in GEOS-4**

Ed Nowotnick
M.S. Scholarly Paper
11/27/2007
Advisors: Dr. Peter Colarco
Dr. Zhanqing Li

Abstract

We have implemented a new dust source scheme in the NASA Goddard Earth Observing System (GEOS-4) atmospheric general circulation model and data assimilation system. By linking our dust source scheme more closely to the surface, the new scheme is a more physically based scheme than previous incarnations of the model. Here we use A-Train observations from MODIS and CALIPSO along with AERONET and NAMMA LASE data to evaluate simulated dust distributions using the new source scheme during 2006.

1. Introduction

Desert dust significantly influences the Earth climate system in a variety of ways. Dust directly forces the Earth's radiation budget through the absorption and scattering of short-wave radiation [Sokolik and Toon, 1996]. Dust indirectly affects the Earth's climate by serving as abundant cloud condensation nuclei, which can act to suppress precipitation [Rosenfeld et al., 2001]. In California, dust was shown to indirectly reduce surface wind speeds and evapotranspiration, leading to a reduction in precipitation [Jacobson and Kaufman, 2006]. The transport of dust composed of iron is essential to ecosystems in the Amazon and biogeochemical processes in the ocean surface [Falkowski et al., 2003, Koren et al. 2006]. Human activity and land use has been shown to have an influence on global dust concentrations as well [Mahowald et al., 2003].

Annually, 240 Tg of dust is transported from North Africa to the Atlantic Ocean and a significant source is the Bodele' depression [Koren et al., 2006]. Highly

concentrated dust plumes are observed to originate from a well-mixed layer of dry, warm air, marked by constant potential temperature named the Saharan Air Layer (SAL) [Prospero and Carlson, 1972]. Due to the thermal contrast between the cool waters of the Gulf of Guinea and the warm land surface of North Africa and the large negative soil moisture gradient, the African Easterly Jet (AEJ) forms as a result of the thermal wind balance [Burpee et al., 1972]. The AEJ advects the SAL westward across the North Atlantic Ocean, delivering North African dust to the Caribbean and the southeast United States [Prospero and Carlson, 1981]. African Easterly Waves (AEW) tend to develop within the AEJ as a result of barotropic instability and can be amplified as a result of latent heating during the early stages of cyclogenesis to form storms [Burpee et al., 1972].

Recently, there has been an increase of interest in studying the interactions of North African dust, AEJ, and the African Monsoon Hydrological Cycle (AMHC). The stability and the extreme dryness of the SAL can serve as a mechanism for precipitation suppression [Carlson and Prospero, 1972]. The AEJ was shown to be responsible for the maintenance of precipitation patterns in West and East Africa [Cook et al., 1999]. There has been some observational evidence linking the suppression of convection and tropical cyclones to North African dust and warm and dry anomalies of the SAL [Dunion et al., 2004, Wong et al., 2006]. Results from Evan et al. [2006] suggest a strong link between variability in the SAL and North Atlantic tropical cyclone activity.

Observational evidence suggests that the radiative effect of dust can amplify AEWs [Jones et al., 2004]. Lidar observations have been used to show detailed spatial relationships between the dust plumes and the dynamical fields [Karyampudi et al.,

1999].

While significant advances have been made in attempting to understand each facet of dust, the sources, distributions, and radiative forcings are still not well understood [Zender et al, 2004]. Previous global model simulations have shown a great range of mean global emission and burden values that are the result of discrepancies in the model source schemes, model and meteorology uncertainties, and discretization [Zender et al., 2004].

The current state of dust modeling signifies that the progression from the modeling of simple to complex processes has made improvements when compared to satellite observations. However, there are still important differences between observations and modeled distributions. Differences may arise from incorrect representations of sources, vertical distributions, and wave dynamics. The current state of dust modeling does not link the dust cycle to climate because it ignores the radiative effect and feedback of dust back into the climate system.

To better understand the role of dust in tropical cyclogenesis, it is first necessary to improve the representation of the dust emission process in global models. In order to explore this problem, the NASA GEOS-4 model will be used to test the sensitivity of dust distributions to a new source scheme when compared to NASA observations.

2. Model Description

2.1 GEOS-4

The NASA GEOS-4 atmospheric general circulation model was developed by the Goddard Modeling and Assimilation Office (GMAO). GEOS-4 is based on the finite-

volume dynamical core with the NASA data assimilation package and the NCAR CCM3 physics package [Kiehl et al., 1996]. The model is highly configurable, with capabilities to run at $0.625^{\circ} \times 0.5^{\circ}$ horizontal resolution, up to 55 hybrid eta levels in the vertical, and 1800s temporal resolution. GEOS-4 runs using the GMAO meteorological dataset, but has the capability to run using other meteorological datasets. GEOS-4 can run in climate, assimilation, and replay modes. In climate mode, the initial conditions are set and the model provides a forecast for a specified time. GEOS-4 has the capability to perform full data assimilations, but for studying dust, running the model in replay mode is more desirable. In replay mode, prior data assimilations are used to save computational costs and time. The replay mode acts as an online model that provides dynamics between analyses that are more internally consistent than in an offline model.

The aerosol package of GEOS-4 uses an implemented version of the Global Ozone Chemistry Aerosol Radiation and Transport (GOCART) model [Chin et al., 2002]. The GOCART model treats five tropospheric aerosol species (dust, sea-salt, black carbon, organic carbon, and sulfate) as tracers that do not interact radiatively. GOCART treats dust as five tracers spanning radius sizes of 0.1-10 μm . The GOCART model originally used the Ginoux dust scheme, however, we have replaced this scheme with one based on the Dust Entrainment And Deposition (DEAD) model for the purposes of this study [Ginoux et al., 2001, Zender et al., 2003]. It should be noted that we are still using the same Ginoux dust source map, shown below (Fig. 1).

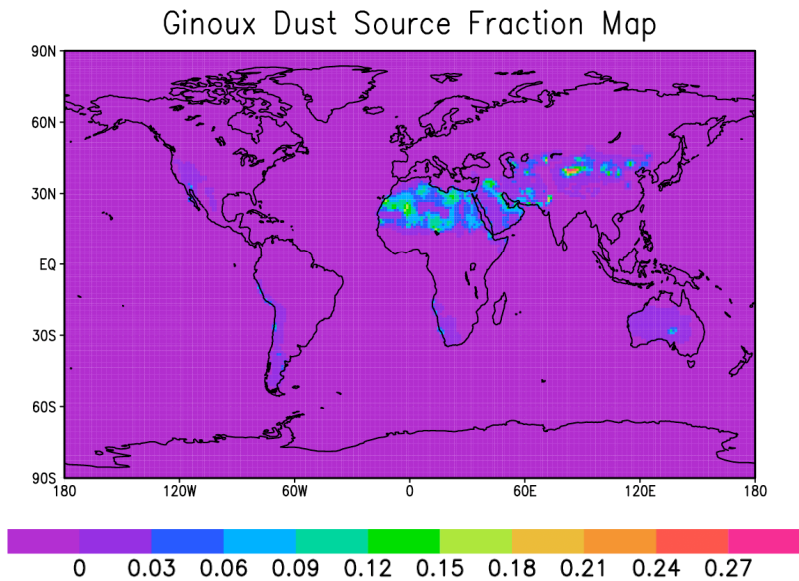


Figure 1- Ginoux source fraction map used by source scheme

2.2 DEAD Scheme

The DEAD source scheme is largely based upon the soil-derived dust emission scheme presented in Marticorena et al., 1995. The DEAD emission process begins with an initial lognormal soil size distribution. For each soil grain size, a semi-empirical function, determined by wind tunnel experiments is used to calculate a threshold friction velocity required to initiate particle movement, or saltation. The threshold friction velocity required for saltation of each grain size is then modified to account for water content and drag partitioning. The presence of water in soils inhibits saltation, thus increasing the threshold friction velocity.

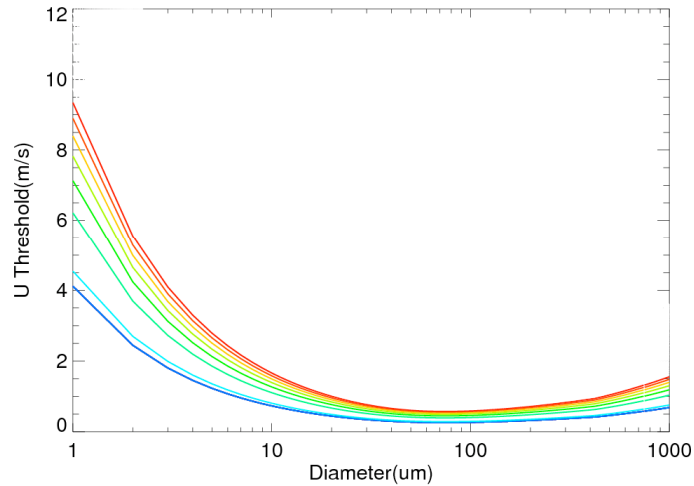


Figure 2 – Effect of water content on threshold friction velocity (blue-0%, red-30% water)

Drag partitioning modifies the threshold friction velocity to represent the presence on non-erodible objects in soil beds. If there are non-erodible objects present, then the roughness length increases, requiring greater energy to initiate saltation. Thus, when drag partitioning is considered, the threshold friction velocity increases. When a particle begins to saltate, there is a transfer of momentum from the bouncing particle back to the ground. This, in effect, is increasing the actual surface friction velocity and is known as the Owen Effect . When the Owen Effect is taken into account, the surface friction velocity increases, making it easier to initiate saltation. Once the threshold friction velocity and surface friction velocity are determined, they are compared to one another. If the surface friction velocity is greater than the threshold friction velocity, then particles of that size begin to saltate. These saltating particles are integrated over a horizontal size distribution to determine the horizontal flux of soil particles. Not all of the saltating particles will be emitted into the atmosphere. In fact, emission is due to the saltating particles bouncing and chipping pieces off of other soil particles, known as sandblasting.

Thus, a conversion factor is used to transfer from the horizontal to vertical flux to represent sandblasting. A lognormal dust particle size distribution is then applied to the vertical flux of soil particles to simulate dust emission.

The old Ginoux scheme is based upon the 10 meter wind speed instead of the surface friction velocity. Dust emission occurs at the surface, making the 10 meter wind speed less ideal for the dust emission parameterization. Thus, we feel that the DEAD scheme better represents the physical process of dust emission because it is tied more closely to the surface.

3. Datasets

To evaluate the new dust source scheme in GEOS-4 observations from several NASA instruments are used. A-Train observations from the Moderate Imaging Spectroradiometer (MODIS onboard Aqua 2002-Present) and the Cloud-Aerosol Lidar with Orthogonal Polarization (CALIOP onboard CALIPSO 2006-Present) provide observations of the same location at nearly the same time. MODIS provides multispectral observations of aerosol properties, with retrievals from 10 channels (7/water and 3/land). For this study, MODIS provided measurements of aerosol optical thickness (AOT) at 550nm. CALIPSO provides measurements of total attenuated backscatter and depolarization ratio at 3 channels at 20.6 Hz. For this study, CALIPSO data was averaged to 1 second increments. Total attenuated backscatter at 532 nm is used to locate aerosol plumes and clouds in the vertical. The depolarization ratio at 532 nm represents the ratio of the perpendicular component of the backscatter to the parallel component. Dust particles are typically non-spherical and give stronger depolarization ratios when compared to other aerosol types, such as sulfates. Data from the Aerosol

Robotic Network (AERONET 1993-Present) is used to supplement A-Train observations by providing measurements of column AOT from the surface at a greater temporal resolution. AERONET sunphotometers face the sun to get information about the spectral AOT and scan the sky to obtain radiances that are used to determine particle size distributions and optical properties. The North African Monsoon Multidisciplinary Analyses (NAMMA) was conducted in August and September 2006 aimed at studying AEWs and tropical convection. Data from the Lidar Atmospheric Sensing Experiment (LASE) flying on the NASA DC-8 during this experiment provides vertical profiles of aerosol scattering ratio, defined as the ratio of aerosol scattering to Rayleigh scattering.

4. Evaluation of Model Simulation

To test the new DEAD source scheme, the year 2006 was simulated because of the alignment of A-Train, AERONET, and NAMMA data. The simulation was performed using all aerosol types at 1x1.25 degree horizontal resolution on 32 hybrid-eta levels in the vertical. All aerosol types were simulated. Presented below are the results of the simulation compared to a simulation using the old Ginoux and the aforementioned NASA observations.

4.1 Comparison to Ginoux Scheme

Fig. 3 and Fig. 4 show monthly means of dust emissions during 2006 for the new DEAD scheme and a simulation using the old Ginoux scheme, respectively. The annual total represents the globally averaged annual mean of dust emissions. Both figures highlight the major source regions of dust on Earth: The Lake Chad region in Africa, the Gobi and Taklamakan deserts in Asia. However, the magnitude of the emissions is quite

different between the two simulations. This is representative of the change in the mobilization process using the DEAD scheme. The DEAD scheme emits much less dust than the Ginoux scheme and appears to be more sensitive to the source map. Note the difference in emissions in April, marked by the red circles.

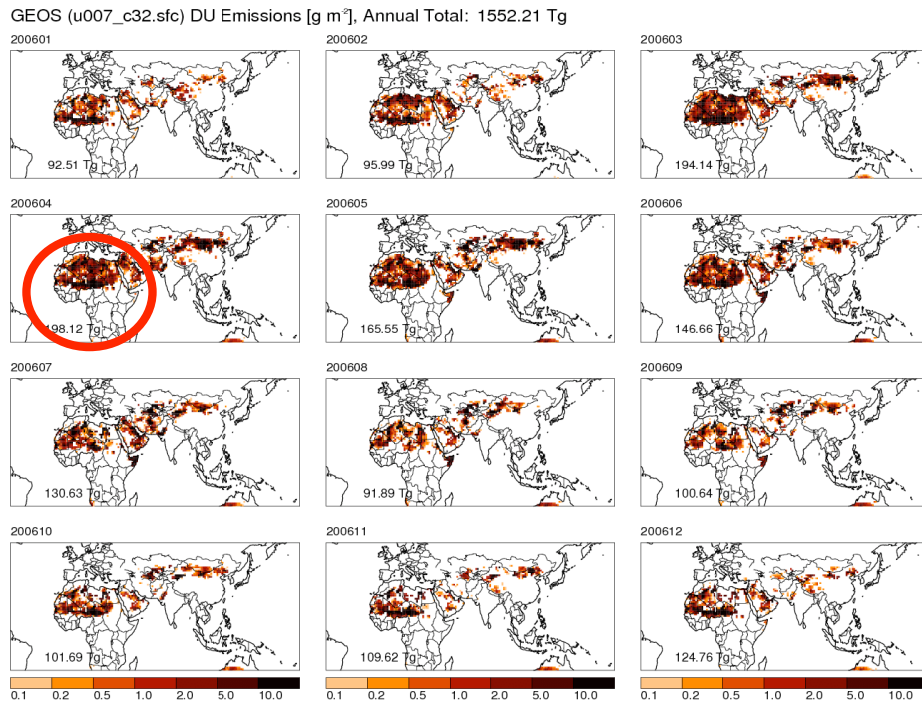


Figure 3 – Monthly mean emissions for 2006 using the new DEAD scheme

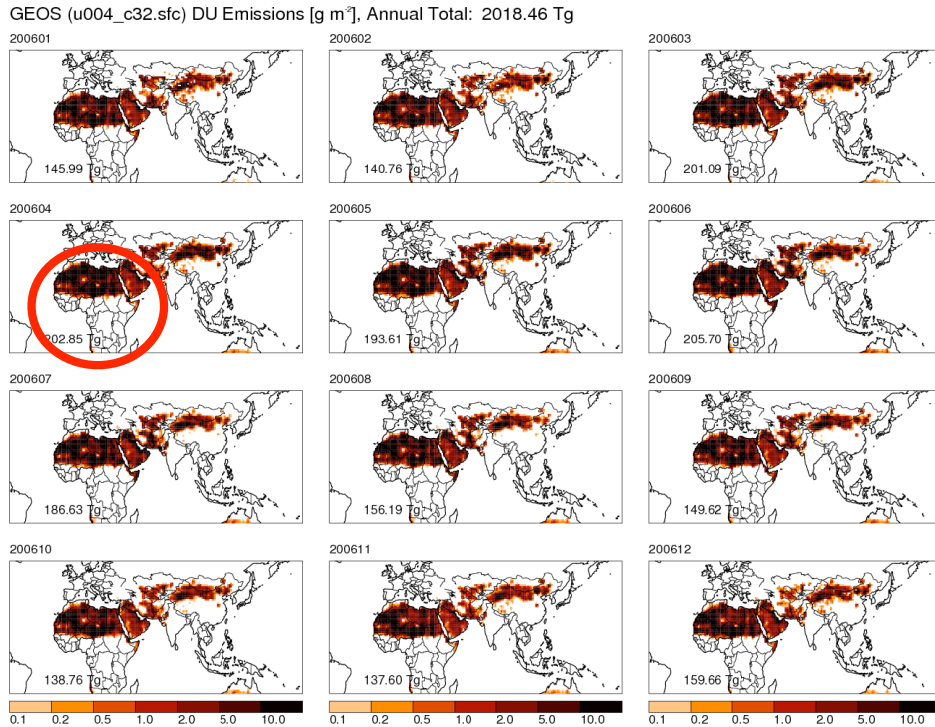
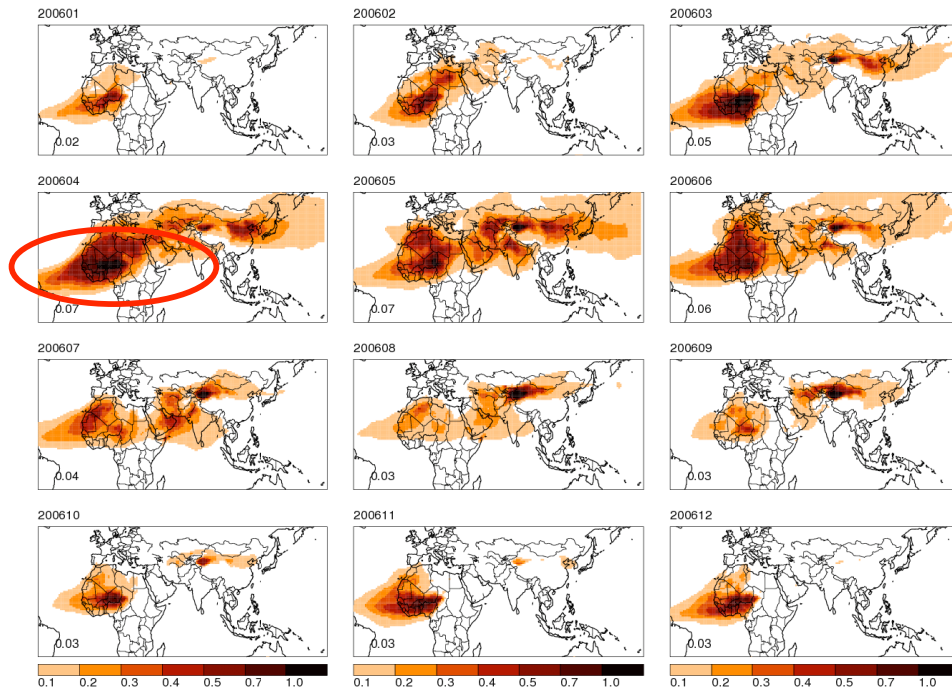


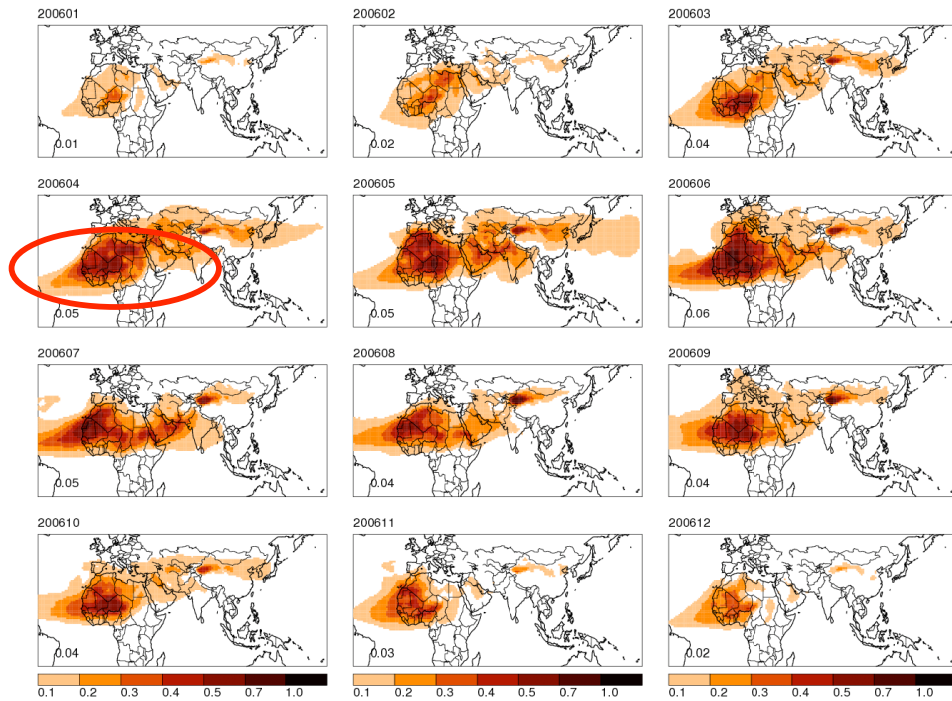
Figure 4 – Monthly mean emissions for 2006 using the Ginoux scheme

Fig. 5 and Fig. 6 show monthly means of dust AOT for the DEAD and Ginoux schemes, respectively. In contrast to the emissions, the AOT values for the two schemes are similar. In April, where the DEAD emissions were much less than the Ginoux emissions, the value of AOT is greater. This is due to the difference in size distributions between the two schemes. The Ginoux scheme emits significant amounts of large ($7\text{-}10\ \mu\text{m}$ in radius) dust particles that fall from the atmosphere quickly and do not contribute much optically. The DEAD scheme does not emit many large particles, hence the low emissions values, but does emit more submicron particles which contribute to the AOT.

GEOS (u007_c32.sfc) DU TAUEXT [550 nm], Annual Average: 0.04



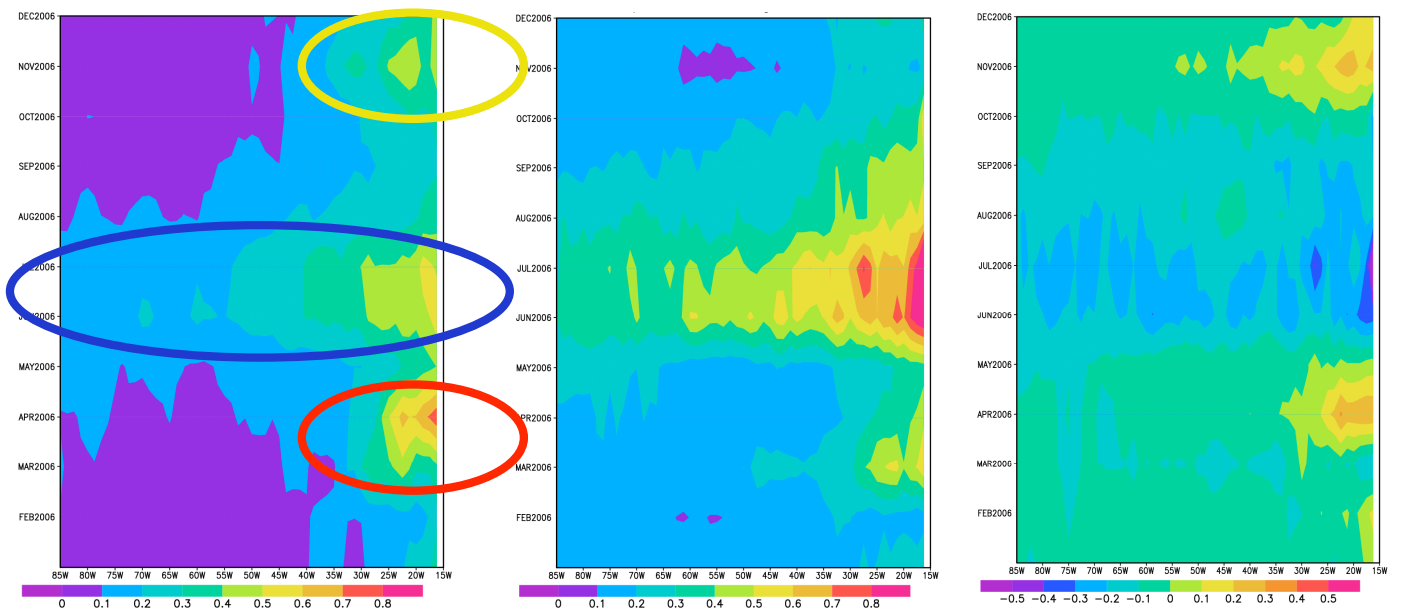
GEOS (u004_c32.sfc) DU TAUEXT [550 nm], Annual Average: 0.04

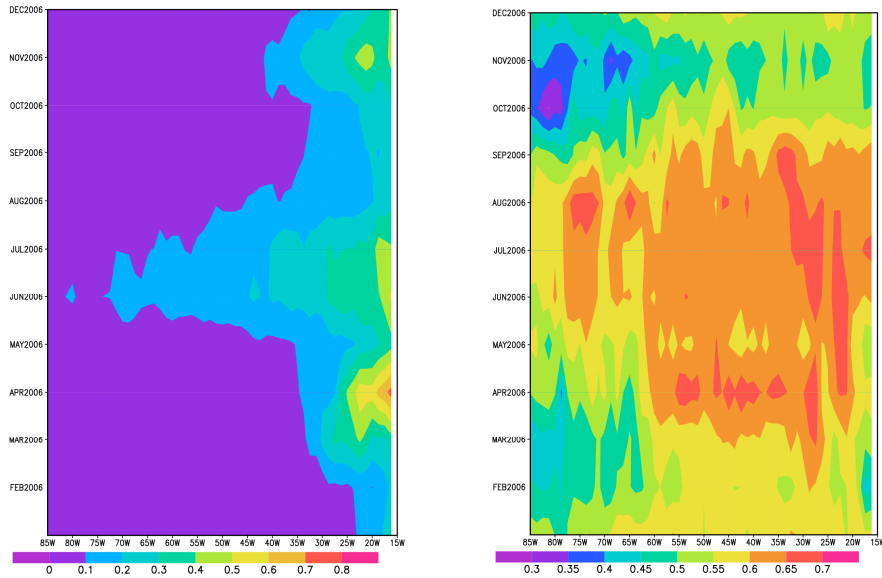


Figures 5 & 6-Monthly means of AOT for 2006 using the new DEAD scheme (top) and the old Ginoux scheme (bottom)

4.2 Comparison to MODIS-Aqua

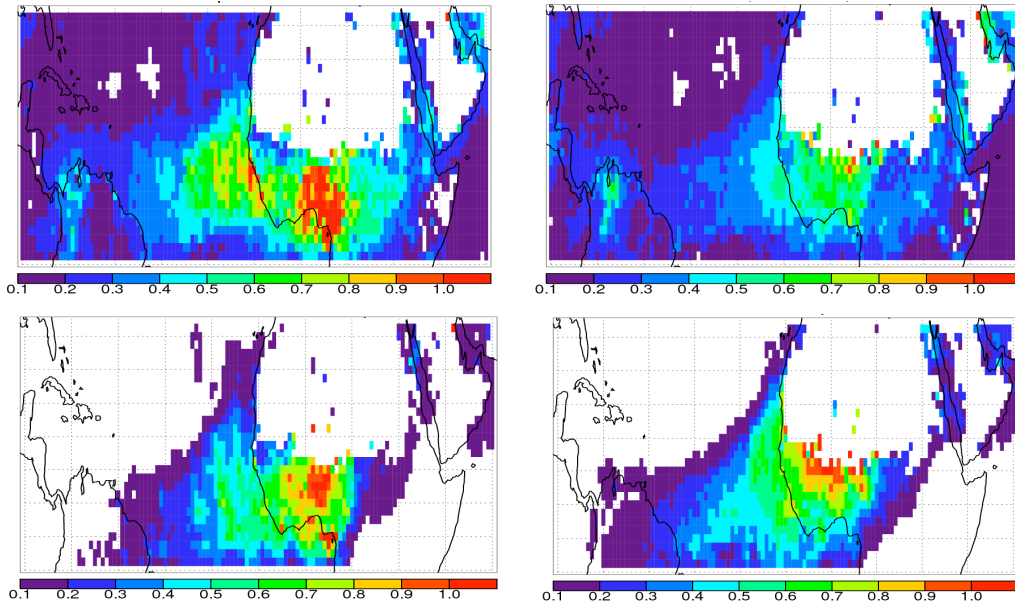
Simulated monthly mean values of AOT averaged from 0-20N from all aerosols (Fig. 7) is similarly compared to monthly mean MODIS-Aqua ocean AOT (Fig. 8). Fig. 9 represents the difference of the simulated AOT from GEOS-4 and the MODIS-Aqua AOT. Fig. 10 shows the simulated AOT from dust only and it is evident from comparing Fig. 7 and Fig. 10 that dust is dominating the AOT plume. Fig. 11 shows the MODIS derived coarse mode fraction. It is evident that the MODIS AOT plume is dominated by large particles, with dust being the most likely aerosol type. The three circles mark significant discrepancies between the model and MODIS. The red circle highlights a dust event(s) simulated in April by GEOS-4 that was not sensed by MODIS. MODIS senses an event in March, but much smaller in magnitude. The blue circle shows that the simulated dust plume does not match the horizontal extent or magnitude of MODIS. The gold circle highlights a dust event simulated by GEOS-4 in November that was sensed by MODIS.



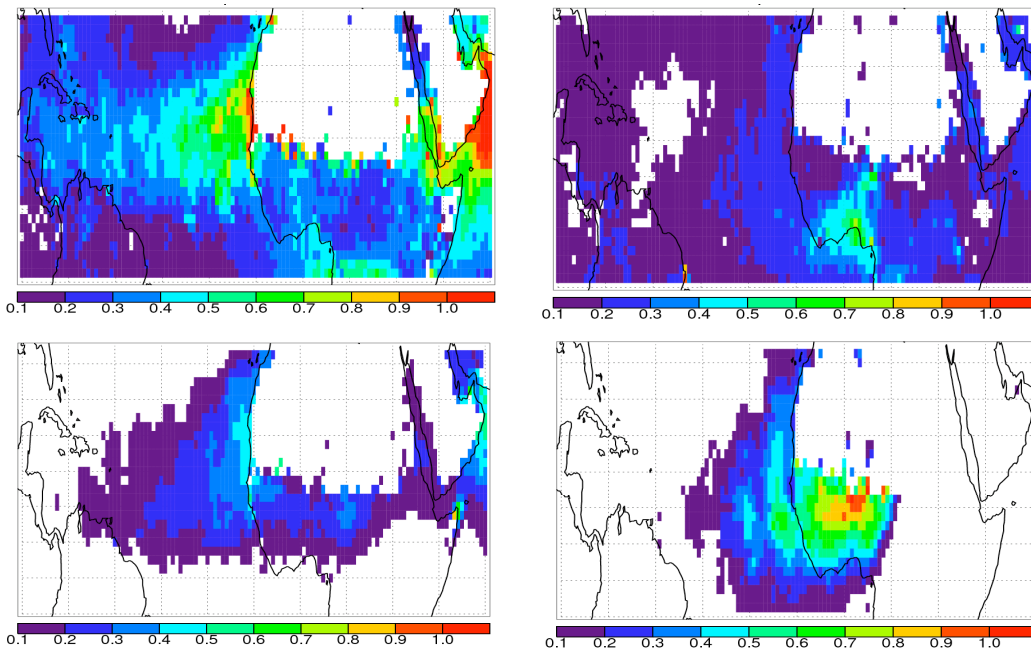


Figures 7-11- GEOS-4 AOT from all aerosols (top, left), MODIS Aqua ocean AOT (top, center), GEOS-4 & MODIS AOT difference (top, right), GEOS-4 AOT from dust only (bottom, left), and MODIS coarse mode fraction (bottom, right)

Figures 12-19 show the spatial distribution of AOT from the MODIS ocean and land products and of the dust component of AOT from GEOS-4 sampled similarly to MODIS for the months of AOT discrepancies. Looking at March, MODIS shows a stronger AOT signal that is directed more to the north than GEOS-4. It should be noted that biomass burning could be contributing to the MODIS AOT, particularly in the Gulf of Guinea region. In April, it is evident that GEOS-4 is producing more dust in the source region than what is seen in the MODIS data and a more pronounced dust plume. During July, MODIS senses a strong AOT signal that extends to the Caribbean. GEOS-4, however, produces much less dust and has the dust plume directed too far to the south. GEOS-4 is emitting large amounts of dust in November that is not seen in the MODIS data.



Figures 12-15-March AOT from MODIS (top, left) and GEOS-4 dust (bottom, left), and April AOT from MODIS (top, right) and GEOS-4 dust (bottom, right)



Figures 16-16-July AOT from MODIS (top, left) and GEOS-4 dust (bottom, left), and November AOT from MODIS (top, right) and GEOS-4 dust (bottom, right)

Several reasons could possibly explain the difference between the MODIS data and the GEOS-4 simulation. One possibility could be that the seasonal cycle of dust emission is not being represented properly in the model. AERONET is used to explore this topic.

4.3 Comparison to AERONET

Six AERONET sites were chosen to compare monthly means of AOT with GEOS-4.

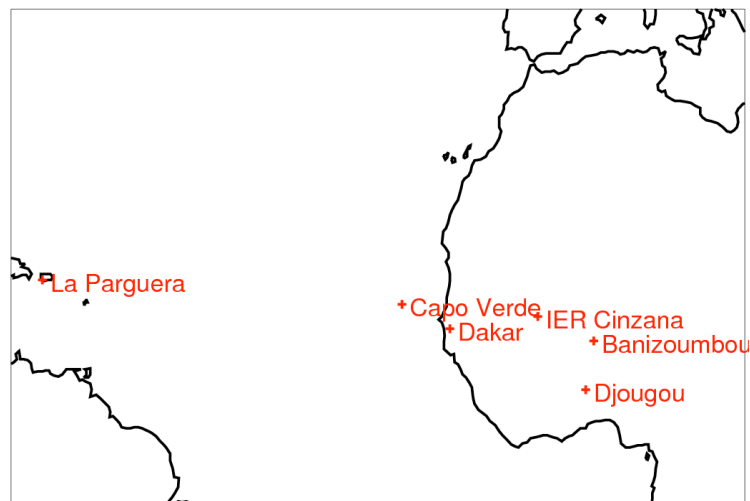
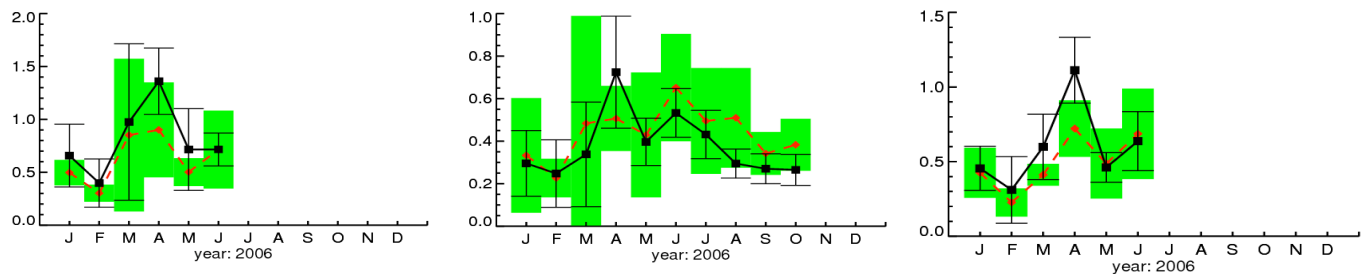


Figure 20-AERONET site locations

Three sites (Banizoumbou-Fig. 21, Dakar-Fig. 22, and IER Cinzana-Fig. 23) were chosen to represent the source region and the other three sites (Cape Verde-Fig. 24, Djougou-Fig. 25, and La Parguera-Fig. 26) represent the transport region. On each figure, the black curve represents GEOS-4 AOT and the red curve represents the AERONET AOT. The bars (black-GEOS-4, green-AERONET) are the standard deviation of the monthly mean. The model was sampled and binned to the nearest AERONET measurement for consistency. In the source region, GEOS-4 matches the seasonal cycle well for every site. However, GEOS-4 consistently simulates too much

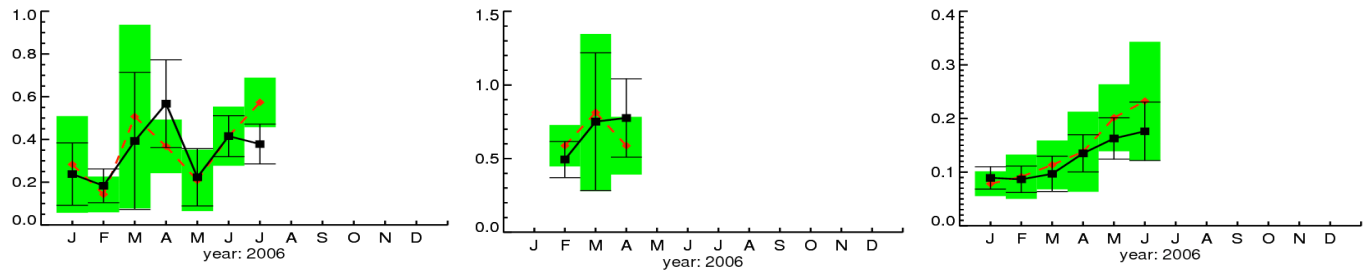
dust in April at every site. This matches what was noticed when GEOS-4 was previously compared to MODIS. In the transport region, both sites near Africa (Cape Verde and Djougou) also match the seasonal cycle well, with the exception of April. The La Parguera site is in Puerto Rico and represents the long distance transport of dust. It is evident that the seasonal cycle is correct, but there is not enough dust being transported during summer months. This was also seen in the MODIS data, where the dust plume was more northern and pronounced than GEOS-4.

Source Region Sites



Figures 21-23-GEOS-4 AOT from all aerosols (black) compared to AERONET AOT (red) for Banizoumbou (left), Dakar (center), and IER Cinzana (right)

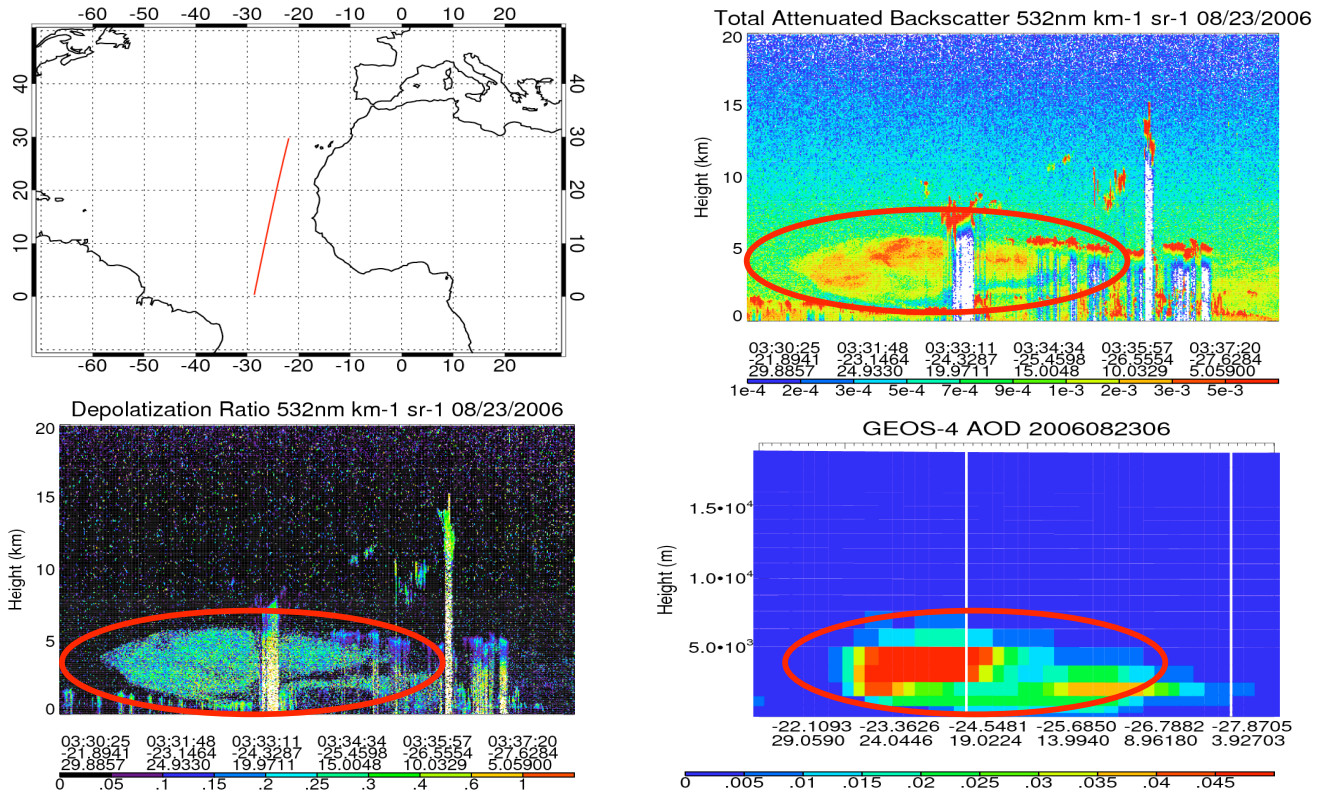
Transport Region Sites



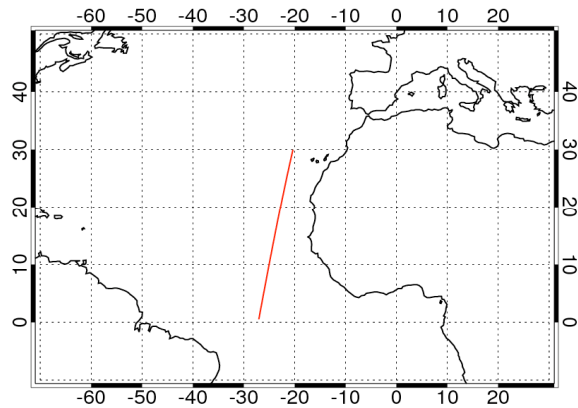
Figures 24-26-GEOS-4 AOT from all aerosols (black) compared to AERONET AOT (red) for Cape Verde (left), Djougou (center), and La Parguera (right)

4.4 Comparison to CALIPSO

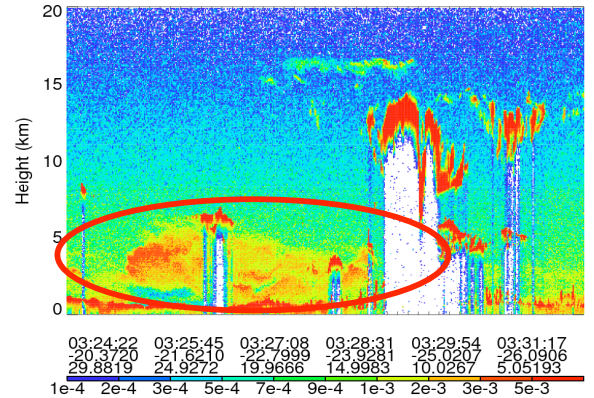
In order to investigate the vertical location of simulated dust plumes in GEOS-4, profiles of total attenuated backscatter from CALIPSO are ideal. Three profiles were chosen as case studies for a qualitative comparison. Profiles of the depolarization ratio are used to distinguish dust from other aerosol types. On each of the three days, the dust plume is distinguished by a red circle. Although GEOS-4 has coarser spatial resolution, GEOS-4 matches well horizontally and vertically when compared to CALIPSO.



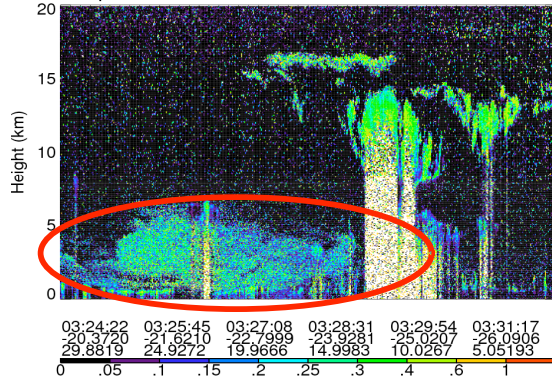
Figures 27-30: CALIPSO track (top, left), CALIPSO Total Attenuated Backscatter (top, right), CALIPSO Depolarization Ratio (bottom, left), and GEOS-4 AOD (bottom, right) for 8/23/2006



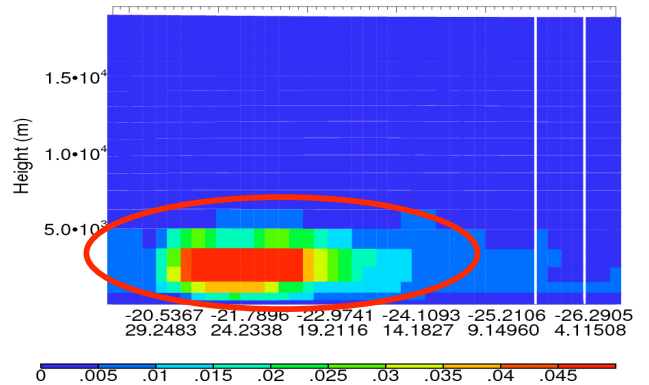
Total Attenuated Backscatter 532nm km-1 sr-1 09/01/2006



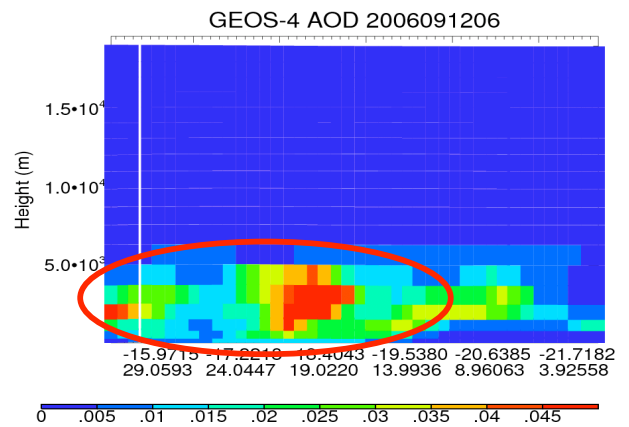
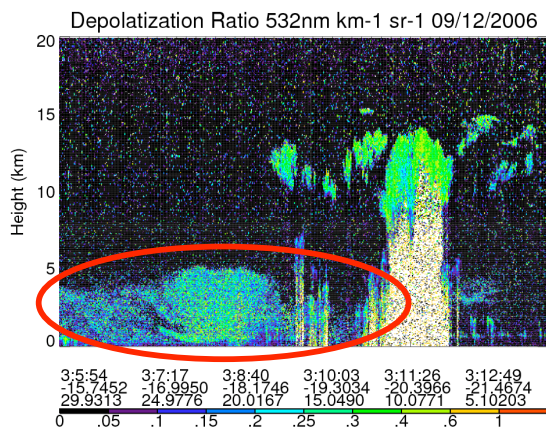
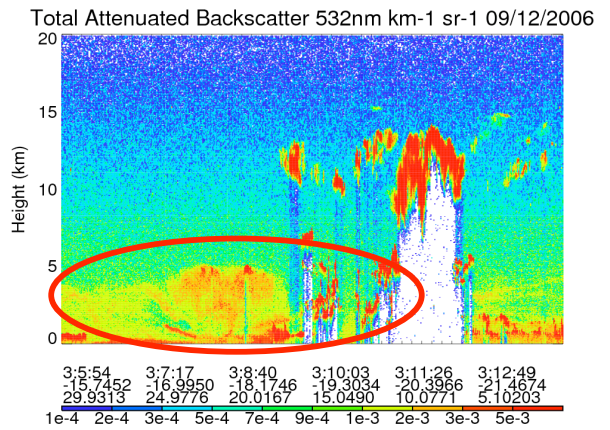
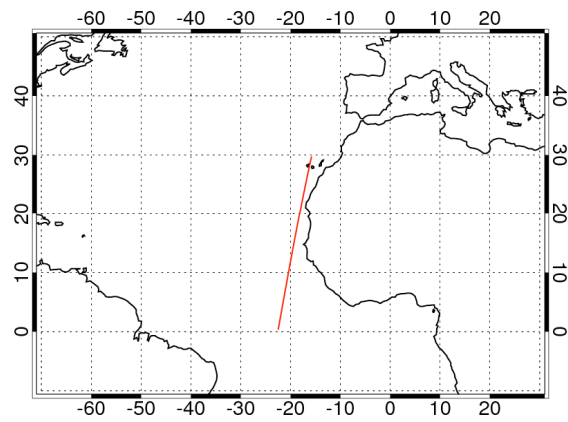
Depolarization Ratio 532nm km-1 sr-1 09/01/2006



GEOS-4 AOD 2006090106



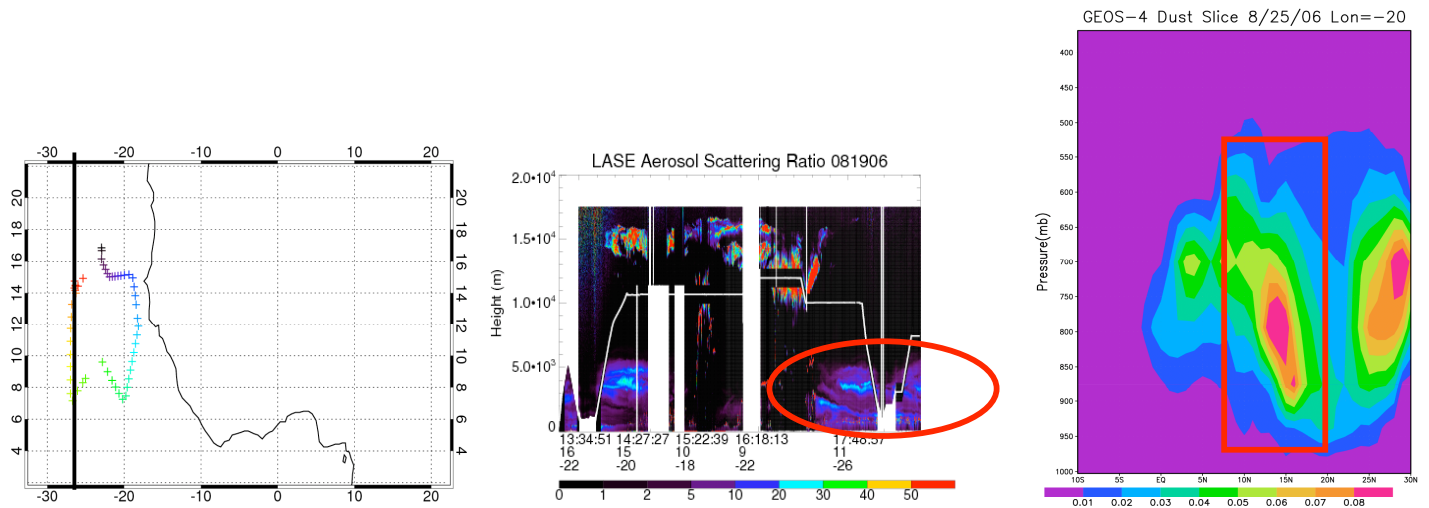
Figures 31-34: CALIPSO track (top, left), CALIPSO Total Attenuated Backscatter (top, right), CALIPSO Depolarization Ratio (bottom, left), and GEOS-4 AOD (bottom, right) for 9/1/2006



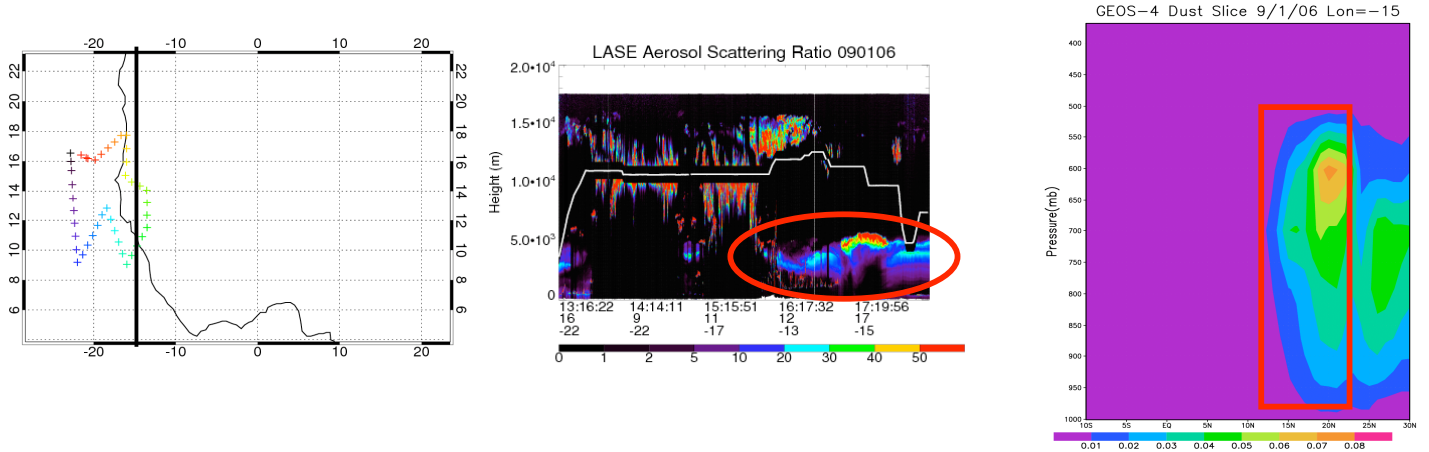
Figures 35-38: CALIPSO track (top, left), CALIPSO Total Attenuated Backscatter (top, right), CALIPSO Depolarization Ratio (bottom, left), and GEOS-4 AOD (bottom, right) for 9/12/2006

4.5 Comparison to NAMMA Field Campaign

Vertical profiles of aerosol scattering ratio from LASE are compared to vertical profiles of AOT from GEOS-4 for two different days. The airplane flight track begins with the black symbols and end with red. The aircraft altitude is shown by the white curves on profiles of aerosol scattering ratio. Black lines through the track represent the longitude slice taken from GEOS-4 for comparison. AOT profiles are on pressure levels making it difficult to compare directly to the LASE data. Nonetheless, on 8/19, GEOS-4 has dust at the same location as the LASE data. On 9/1, GEOS-4 AOD matches the profile of aerosol scattering ratio from LASE again.



Figures 39-41- CALIPSO track (left), CALIPSO aerosol scattering ratio (center), and GEOS-4 AOD (right) on 8/19/2006



Figures 42-44- CALIPSO track (left), CALIPSO aerosol scattering ratio (center), and GEOS-4 AOD (right) on 9/1/2006

5. Summary

The implementation of the new DEAD dust source scheme in GEOS-4 compares well with observations from MODIS, CALIPSO, AERONET, and NAMMA. MODIS data suggests that the simulated dust plume is too far to the south during summer months. One possible reason could be that the assimilated meteorology is incorrect, transporting dust to the wrong location. GEOS-4 has the capability to run with other meteorological datasets, so this topic will be explored. Another possibility is that the dust is being lifted to the incorrect altitude where large scale dynamics control its path. From the CALIPSO case studies, it appears that this is not an issue. The MODIS summer dust plume has a greater magnitude than the simulated dust plume. It is possible that the optical properties of dust in the model is incorrect and does not contribute enough to the total AOT. Additionally, GEOS-4 may not have enough sub-micron sized dust particles, which could explain the smaller magnitude of AOT.

Comparisons to AERONET showed that GEOS-4 simulates the seasonal dust cycle correctly at most locations, although April was too high at all African sites. Optical

properties in the model could be responsible for this as well. The La Parguera site showed that not enough dust is being transported across the Atlantic Ocean in summer months. The assimilated meteorology in GEOS-4 could be an explanation for this feature.

Case studies from CALIPSO and NAMMA LASE show that dust is being lifted to the correct altitude in the model. The horizontal location of simulated dust matches the CALIPSO and LASE data as well. More case studies are necessary to further investigate this issue.

6. References

- Burpee, R., The origin and structure of easterly waves in the lower troposphere of North Africa, *Journal of the Atmospheric Sciences*, Vol. 29, No. 1, pp. 77–90, 1972.
- Cakmur R. V., R. L. Miller, O. Torres (2004), Incorporating the effect of small-scale circulations upon dust emission in an atmospheric general circulation model, *J. Geophys. Res.*, 109, D07201, 2003.
- Chin, M., P. Ginoux, S. Kinne, O. Torres, B. Holben, B. Duncan, R. Martin, J. Logan, A. Higurashi, T. Nakajima, Tropospheric aerosol optical thickness from the GOCART model and comparisons with satellite and sun photometer measurements, *Journal of the Atmospheric Sciences*, Vol. 59, No. 3, pp. 461–483, 2002.
- Cook, K. H., Generation of the African easterly jet and its role in determining West African precipitation. *J. Climate*, 12, 1165–1184, 1999.
- Dunion, J., C. Velden, The impact of the Saharan air layer on Atlantic Tropical Cyclone Activity, *Bull. Am. Meteor. Soc.*, 85, 353-365, 2004.
- Evan A. T., J. Dunion, J. A. Foley, A. K. Heidinger, C. S. Velden (2006), New evidence for a relationship between Atlantic tropical cyclone activity and African dust outbreaks, *Geophys. Res. Lett.*, 33, 2006.
- Falkowski, P., R. Barber, V. Smetacek, Biogeochemical controls and feedbacks on ocean primary productivity, *Science*, 281, pp. 200-206, 1998.
- Ginoux, P., M. Chin, I. Tegen, J. M. Prospero, B. Holben, O. Dubovik, S.-J. Lin, Sources and distributions of dust aerosols simulated with the GOCART model, *J. Geophys. Res.*, 106(D17), 20255-20274, 2001.
- Jones C., N. M. Mahowald, C. Luo, Observational evidence of African desert dust intensification of easterly waves, *Geophys. Res. Lett.*, 31, L17208, 2004.
- Karyampudi, V. M., S. Palm, J. Reagen, H. Fang, W. Grant, R. Hoff, C. Moulin, H.

- Pierce, O. Torres, E. Browell, S. Melfi, Validation of the Saharan dust plume conceptual model using LIDAR, Meteosat, and ECMWF Data, *Bulletin of the American Meteorological Society*, Vol. 80, No. 6, pp. 1045–1075, 1999.
- Kiehl, J. T., J. J. Hack, G. B. Bonan, A. Boville, B. P. Briegleb, D. L. Williamson, P. J. Rasch, Description of the NCAR Community Climate Model (CCM3)., NCAR Technical Note, NCAR/TN-420+STR, Boulder, CO, 152pp, 1996.
- Mahowald N. M., C. Luo, A less dusty future?, *Geophys. Res. Lett.*, 30 (17), 1903, 2003.
- Marticorena B., G. Bergametti, Modeling the atmospheric dust cycle: 1. Design of a soil derived dust emission scheme, *J. Geophys. Res.*, 1995.
- Prospero, J. M., T. N. Carlson, Saharan air outbreaks over the tropical North Atlantic, *Pure Appl. Geophys*, 119, 677-691, 1981.
- Prospero, J. M., T. N. Carlson, Vertical and areal distribution of Saharan dust over the western equatorial North Atlantic Ocean, *J. Geophys. Res.*, 77, No. 27, 5255-5265, 1972.
- Rosenfeld, D., Y. Rudich, and R. Lahav, Desert dust suppressing precipitation: A possible desertification feedback look, *Proc. Nat. Acad. Sci.*, 98 (11), 5,975-5,980, 2001.
- Sokolik, I. N., and O. B. Toon, Direct radiative forcing by anthropogenic airborne mineral aerosols, *Nature*, 381, 681-683, 1996.
- Wong S., P. R. Colarco, A. E. Dessler (2006), Principal component analysis of the evolution of the Saharan air layer and dust transport: Comparisons between a model simulation and MODIS and AIRS retrievals, *J. Geophys. Res.*, 111, 2006.
- Zender C. S., H. Bian, D. Newman, Mineral Dust Entrainment and Deposition (DEAD) model: Description and 1990s dust climatology, *J. Geophys. Res.*, 108 (D14), 4416, 2003.
- Zender, C., R. Miller, I. Tegen (2004), Quantifying Mineral Dust Mass Budgets: Terminology, Constraints, and Current Estimates, *Eos Trans. AGU*, 85(48), 509, 10,2004.